Desalination and Water Treatment
www.deswater.com
doi: 10.1080/19443994.2015.1041051

57 (2016) 9776–9788
May

Taylor & Francis
Taylor & Francis Group

Removal of chromium (VI) from aqueous solution using modified CdO nanoparticles

Ashok V. Borhade[a,*], Bhagwat K. Uphade[b]

[a]*Research Center, Department of Chemistry, HPT Arts and RYK Science College, Nasik 422005, India, Tel. +91 9421831839; email: ashokborhade2007@yahoo.co.in*
[b]*Research Center, Department of Chemistry, P.V.P College, Pravaranagar 413713, India, Tel. +91 9422741036; email: bk_uphade@rediffmail.com*

Received 16 July 2014; Accepted 19 March 2015

ABSTRACT

The CdO and modified CdO nanoparticles were synthesized using hydrothermal method. The absorption spectra, crystal phase, surface morphology, particle size, and surface area of CdO and modified CdO nanoparticles were studied by UV–DRS, FT-IR, XRD, SEM, TEM, TGA, PL, and BET surface area analysis. The present paper reports adsorption technique for the removal of chromium (VI) using CdO and modified CdO nanoparticles. The operating variables such as adsorbent dose, nature of adsorbent, adsorbate concentration, contact time, and pH were optimized. The technique was found to be highly useful and cost effective for removal of chromium (VI). The Langmuir and Freundlich models were evaluated using the experimental data and result showed that the Freundlich isotherm fit better than the Langmuir isotherm.

Keywords: Hydrothermal synthesis; CdO nanoparticles; Modified CdO nanoparticles; Adsorption; Chromium (VI)

1. Introduction

Cadmium oxide nanomaterial is an II–VI *n*-type of semiconductor with a direct band gap of 2.5 eV [1] and 1.98 eV an indirect band gap [2]. The physical and chemical properties of CdO nanoparticles are relative to its stoichiometry as well as particle size, shape which depend on its preparation methods and condition [3]. Cadmium oxide nanoparticles have been synthesized by several methods [4–11]. The physical and chemical properties of cadmium oxide nanomaterials were improved by modifying the synthesis methods [12]. Hydrothermal method found to be a beneficial technique to prepare various nanostructures among the other methods [13]. Cadmium oxide nanoparticles have interesting properties such as large band gap, low electrical resistivity, and high transmission in the visible region. A cadmium oxide nanoparticles have distinguished properties [14] so is widely used as transparent conductive oxide in optoelectronic devices [15], nonlinear materials, and catalysts [16]. The modified CdO nanoparticles are used as sensor for the study of biologically active compounds [17]. Cadmium oxide nanomaterials have been reported as an antibacterial agent [18]. Cadmium oxide nanoparticles are nontoxic, chemically stable under high temperature, and capable

*Corresponding author.

of photocatalytic oxidation [19]. The cadmium oxide nanocrystalline material is also used as catalyst in organic transformation like acylation of alcohols, phenols, and amines [20]. Recently, the removal of heavy metal using nanomaterial has been focused due to its high surface area [21,22].

The chromium (VI) was removed using walnut hull [23], hazelnut and almond shell [24], agaricus bisporus [25], lignin-based resin [26], acidic chloride media using solvent impregnated resin [27], low-cost dolomite [28], marine isolates of yarrowia lipolytica [29], amine functionalized natural and acid activated sepiolites [30], chitosan and single/multi-walled carbon nanotubes [31], polyacrylonitrile/polypyrrole core/shell nanofiber [32], biochars obtained during biomass pyrolysis [33], thiocarbamoyl chitosan [34], diethylene triamine-grafted glycidyl methacrylate-based copolymers [35], nanosized metal oxides [36], amine cross-linked wheat straw [37], low-cost fertilizer industry waste material [38], chrysophyllum albidum (sapotaceae) seed shells [39], activated carbon [40], synthetic adsorbents [41], Lewatit-anion exchange resins [42], ion exchange resins [43], natural adsorbents [44], nanosized ferric oxyhydroxide-loaded anion exchanger [45], green coconut shell [46], porous α-$Fe_2O_3/Fe_3O_4/C$ [47], alginate-montmorillonite/polyaniline nanocomposites [48], magnetic graphene oxide nanocomposites [49], and tunisian clay [50].

Chromium (VI) is harmful even in small intake quantity whereas chromium (III) is considered essential for good health in moderate intake and an essential nutrient [51]. If chromium concentrations are high then it causes stomach ulcers, immunological effects, dizziness, headache, weakness, dermal disease, damage to lung and carcinogenic disease [52]. The compounds of chromium are known to be harmful to human health, the maximum level permitted in waste water is 5 ppm for trivalent chromium and 0.05 ppm for hexavalent chromium [53,54]. Chromium (VI) will penetrate the skin 10,000 times faster than chromium (III) which causes dermal disease and damage to lung. While combustion of coal and oil also release large quantities of "chromium" into the environment. Therefore, it is necessary to remove chromium (VI) from wastewater.

In the present study, the removal of chromium (VI) by the synthesized CdO and modified CdO nanoparticles was investigated. The removal of chromium (VI) from aqueous solution at different pH, amount of CdO or modified CdO nanoparticles, contact time, and different initial concentration of chromium (VI) was studied.

2. Materials and methods

2.1. Synthesis of CdO nanoparticles

The CdO nanoparticles were synthesized by hydrothermal method [55] in which cadmium chloride (1.0 mmol), methanol (0.1 mmol), and triton X-100 (1.0 mmol) was homogenized properly in a round bottom flask. In this reaction mixture, sodium hydroxide (0.1 M) was slowly added and the reaction mixture was stirred for 2 h at room temperature. The reaction mixture was filtered with Gooch crucible and nanocrystalline cadmium oxide obtained was washed with distilled water. The cadmium oxide was dried in oven at 110˚C and further calcinized at 400˚C for 4 h.

2.2. Synthesis of modified CdO nanoparticles

The synthesized cadmium oxide nanoparticles were used as precursor material and cesium nitrate as dopant for the synthesis of Cs-doped CdO nanoparticles. Initially, cadmium oxide (1.0 mol) nanoparticles were mixed with 3 and 7% cesium nitrate solution along with sodium hydroxide (2.0 M). The slurry obtained was stirred well and transferred into Teflon autoclave and kept in oven at 110˚C for 20 h. The precipitate obtained was vacuum filtered, washed with distilled water for the removal of soluble impurities, and dried at 110˚C for 2 h. This precipitate was calcinized at 400˚C for 2 h and used for characterization. The synthesized CdO and modified CdO nanoparticles were used for the removal of chromium (VI) from aqueous solution.

The potassium dichromate (Loba Chemie, 99.5%), sulfuric acid (Loba Chemie, 91%), and sodium hydroxide (Sigma Aldrich, 98.5%) were used for the study. Potassium chromate was used as a heavy metal source of chromium (VI), synthesized CdO, modified CdO nanoparticles were used in this investigation. The desired pH of the solution was maintained by the use of previously standardized sulfuric acid (2.0 M) and sodium hydroxide solution (2.0 M). The progress of removal of chromium (VI) was followed by measuring absorbance using UV–visible spectrophotometer.

2.3. Removal of chromium (VI)

For removal of chromium (VI), 50 ml of chromium (VI) solution and the adsorbents (CdO or modified CdO nanoparticles) were taken in a beaker. The chromium solutions were mixed properly and the absorbance of chromium solution was recorded at 435 nm using UV–visible spectrophotometer. The removal of

chromium (VI) was evaluated at different pH, different initial concentrations of chromium, contact time, and various amount of CdO and modified CdO nanoparticles as adsorbent.

3. Results and discussion

3.1. Characterization of CdO and modified CdO nanoparticles

3.1.1. UV–DRS analysis

The UV–DRS spectra of the CdO, 3 and 7% Cs doped CdO nanoparticles are shown in Fig. 1. The spectra show broadband at 340, 346, and 353 nm for CdO, 3 and 7% Cs doped CdO nanoparticles, respectively. The blue shift observed as compared to bulk CdO is due to quantum confinement effects. With increase in the amount of the dopant, the band position shifted to higher wavelength side. The band gap energies of the synthesized CdO, 3 and 7% Cs-doped CdO nanoparticles are 3.64, 3.58, and 3.52 eV, respectively. The shifting of band is arising due to doping of Cs in CdO nanoparticles.

3.1.2. FT-IR analysis

Fig. 2 depicts FT-IR spectra for the synthesized CdO, 3 and 7% Cs-doped CdO nanoparticles in KBr matrix. The absorption bands at 3,523 cm^{-1} are attributed to the stretching vibration of the -OH group due to small amount of water adsorbed on the surface of CdO nanoparticles [56]. The strong broad absorption band at about 1,408 cm^{-1} is due to the asymmetric stretching vibrations of water molecule [57]. The broad absorption band at 858 cm^{-1} shows the presence of Cd-O bond [58]. The FT-IR spectra shows absorption band at 501 cm^{-1} also confirms the presence of Cd-O bond [59] and frequency at 1,000 cm^{-1} is due to oxygen stretching. The absorption band at 501 cm^{-1} becomes broad due to the presence of cesium ion in CdO nanoparticles.

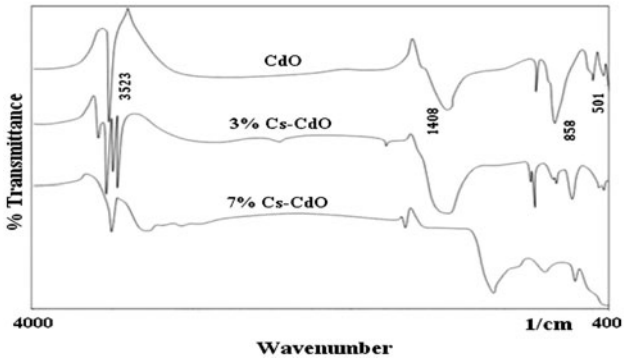

Fig. 2. FT-IR spectra of synthesized CdO, 3 and 7% Cs-doped CdO nanoparticles.

3.1.3. X-ray diffraction (XRD) analysis

Fig. 3 shows XRD pattern of synthesized CdO, 3 and 7% Cs-doped CdO nanoparticles. The diffraction peaks indicate the nanocrystalline nature of synthesized CdO and peaks at 2θ values of 15.4, 17.2, 29.4, 31.06, 35.08, 38.7, 39.5, and 43.06 corresponds to the reflection from 111, 200, 311, 222, 400, 331, 420, and 422 crystal planes. The XRD pattern is in agreement with cubic structure of CdO nanoparticles (JCPDS card No. 02-1102) indicated the formation of cadmium oxide phase. Sharp diffraction peak indicates good crystallinity of CdO nanoparticles and XRD patterns show obvious size broadening effects due to small crystallite size. It can be found that cesium doping do not change crystalline structure of CdO nanoparticles. The particle size is found to be 47, 44, and 41 nm for

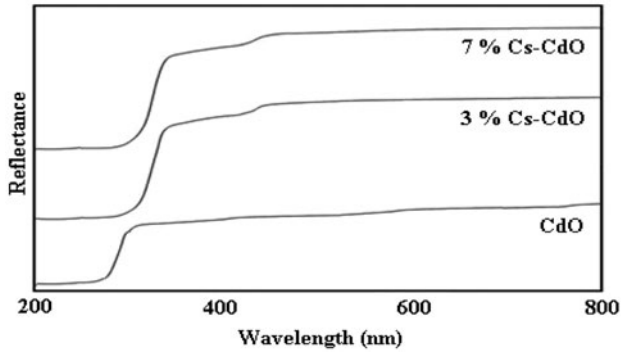

Fig. 1. UV–DRS spectra of synthesized CdO, 3 and 7% Cs-doped CdO nanoparticles.

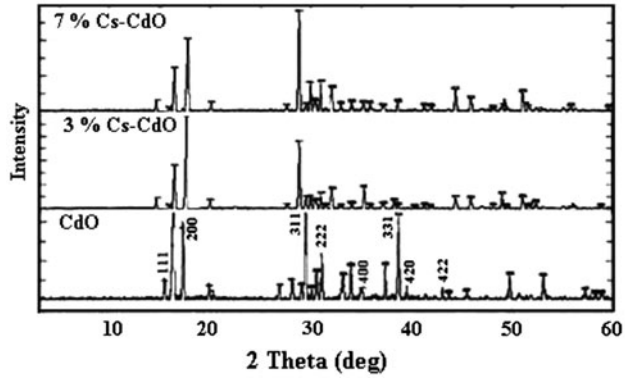

Fig. 3. XRD pattern of synthesized CdO, 3 and 7% Cs-doped CdO nanoparticles.

CdO, 3% Cs-doped CdO, and 7% Cs-doped CdO nanoparticles [60]. In comparison with pure CdO nanoparticles, the cesium-encapsulated CdO has relatively small particle size indicating that the doping can improve the morphology and retard the grain growth of CdO nanoparticles.

3.1.4. SEM and EDAX analysis

The SEM images along with EDAX of synthesized CdO, 3 and 7% Cs-doped CdO samples are presented by Fig. 4. The morphology of the CdO nanoparticles is cubic in nature with agglomerates while 3 and 7% Cs-doped CdO nanoparticles show rod-like structure along with cubic morphology. The average particle size varies in the range of 47–41 nm as measured using the XRD patterns. Strong peaks of Cd and O are found in the EDAX spectrum and also definite amount of cesium indicate that cesium ion has doped into CdO nanoparticles. The EDAX spectrum shows that 2.98 and 6.93% of cesium ion is present in the Cs-doped CdO nanoparticles which indicate the

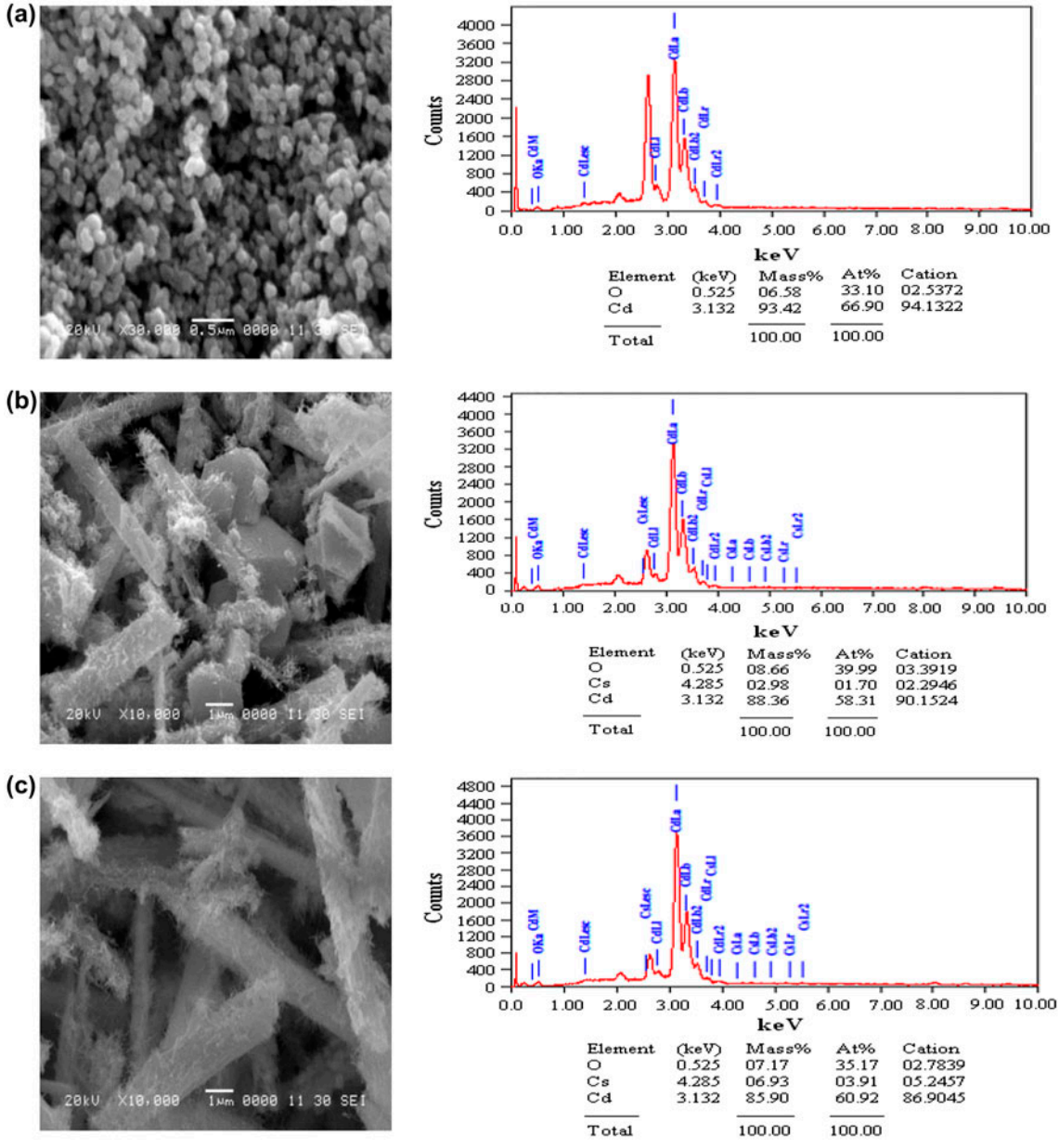

Fig. 4. SEM and EDAX of (a) synthesized CdO, (b) 3% Cs-doped CdO, and c) 7% Cs doped CdO nanoparticles.

doping of cesium ion into the nanocrystalline CdO material. The slight decrease in the amount of cesium in Cs-doped CdO nanoparticles is due to the washing.

3.1.5. TEM and SAED analysis

The size and morphological information of the sample was investigated by TEM with SAED analysis and are depicted in Fig. 5. The TEM image of CdO nanoparticles shows the cubic structure, while 3% or 7% Cs-doped CdO nanoparticles show rod-like structure along with cubic morphology. Moreover, the particle size of the synthesized CdO nanoparticles obtained from TEM analysis is similar to those estimated from Debye– Scherrer's equation [60] and in the range of 47–41 nm. The dark spot in the TEM image can be alluded to the synthesized CdO, 3 and 7% Cs-doped CdO nanoparticles as SAED pattern associated with such spot reveals the occurrence of CdO, 3 and 7% Cs-doped CdO nanoparticles in total agreement with the XRD data. The SAED pattern of CdO, 3 and 7% Cs-doped CdO nanoparticles show similar *d*-values as obtained from XRD data.

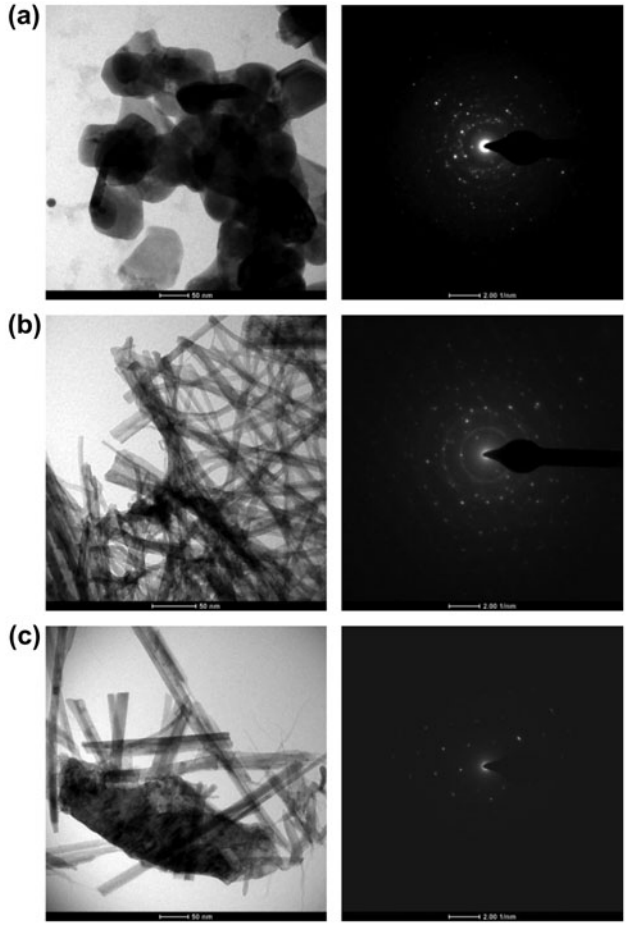

Fig. 5. TEM and SAED of (a) synthesized CdO, (b) 3% Cs-doped CdO, and c) 7% Cs doped CdO nanoparticles.

3.1.6. Thermogravimetric analysis (TGA)

Fig. 6 illustrates the curve of TGA of the CdO nanoparticles. TGA curve shows the decomposition of CdO nanoparticles is performed in a two-step pattern of the weight loss. The first weight loss of 2.743% is observed in the range of temperature between 279.23 and 314.84˚C, which can be related to decomposition of adsorbed water molecules. The second weight loss of 1.947% is observed in the temperature range 314.84–374.90˚C can be associated with decomposition of the organic contents in the precursor. It was found that the weight loss terminates at 400˚C and stable in 400–500˚C, so this temperature was determined as the calcinations temperature of the intermediate molecules and reaching the CdO phase.

3.1.7. Photoluminescence analysis (PL)

The PL spectrum of the CdO nanoparticles shows blue shift in relation to the bulk and the band gap (bulk CdO, 538 nm) is shown by Fig. 7. The emission wavelength of the CdO nanoparticles is at ~563 nm (E = 2.2 eV), dependent on the particle size (quantum size effect) which is the band edge or near band edge emission and considered due to transition between valence and the conduction band. The relatively large width of the emission band of the CdO nanoparticles is due to the broad distribution of intraband states associated with different trapping sites. The blue shift in the excitation absorption reflects the correspondingly

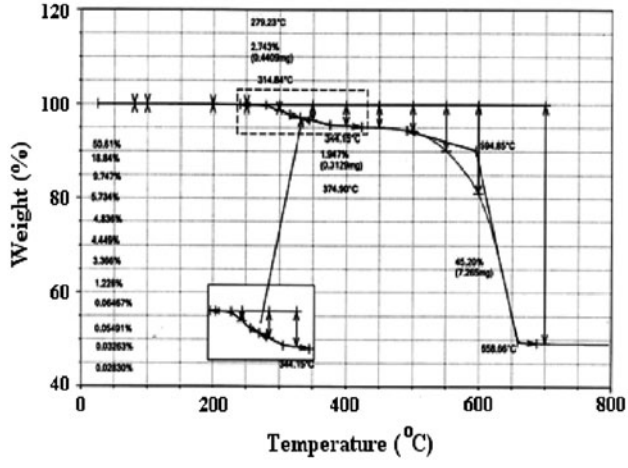

Fig. 6. TGA curve of synthesized CdO nanoparticles.

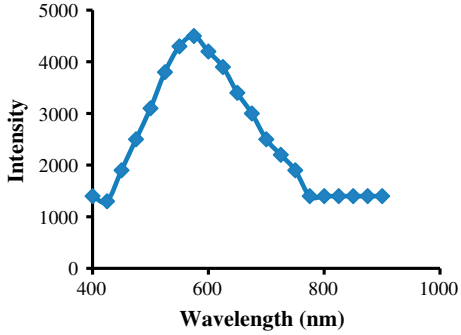

Fig. 7. Photoluminescence spectrum of synthesized CdO nanoparticles.

gradual removal of the initial trap and surface states during the crystallization process of nanoparticles. By controlling the morphology, the optical property of CdO nanostructures can be tunable which will be useful for the photodegradation applications.

3.1.8. BET surface area analysis

The BET surface area measurement curves for synthesized CdO, 3 and 7% Cs-doped CdO nanoparticles are shown in Fig. 8(a)–(c). The N_2 adsorption–desorption isotherms and BJH pore size distribution of CdO nanoparticles reveals that the sample has typical IV N_2 adsorption–desorption isotherms with H_1 hysteresis and has a narrow pore diameter range. Based on the N_2 adsorption–desorption isotherms the specific surface area (S_{BET}) of CdO nanoparticles is 29.71 m^2/g, the average pore volume (V_P) and pore diameter (d_p) were 0.04630 cc/g and 24.87 Å, respectively. In 3 and 7% Cs-doped CdO nanoparticles, the specific surface area (S_{BET}) obtained from BET method is 36.27 and 57.13 m^2/g, the average pore volume (V_P) and pore diameter (d_p) were 0.04832 cc/g, 0.05769 cc/g, and 30.92 Å, 31.09 Å, respectively. The modified CdO nanoparticles have large surface area, average pore volume, and pore diameter than pure CdO nanoparticles.

3.2. Removal of chromium (VI)

Adsorption process assisted by CdO and modified CdO nanoparticles depend on various parameters like initial concentration of chromium (VI), concentration and nature of the adsorbent, pH, contact time, and temperature [61]. The absorbance of the chromium (VI) solution was measured before and after removal using UV–visible spectrophotometer. From the respective absorbance, percentage removal of chromium was calculated using the equation,

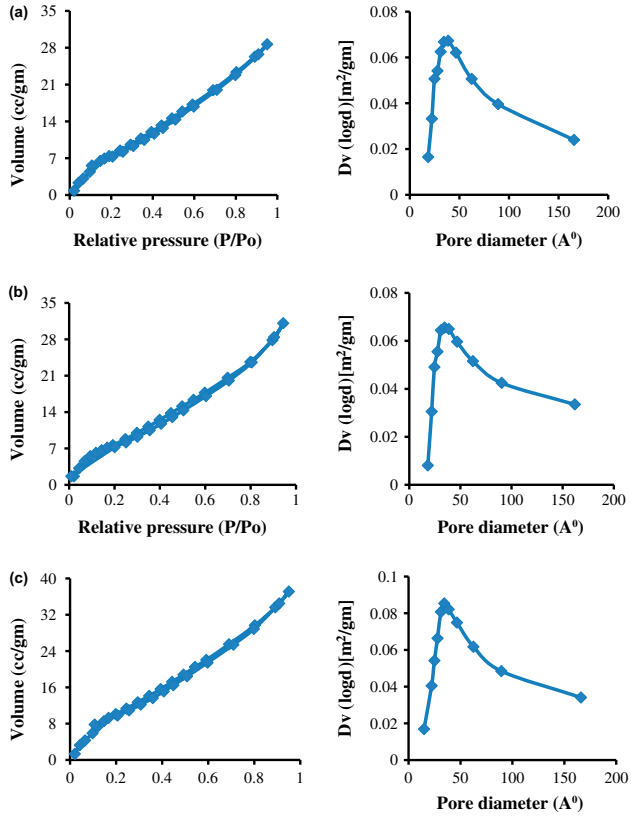

Fig. 8. BET surface area and pore size of (a) synthesized CdO, (b) 3% Cs-doped CdO, and (c) 7% Cs doped CdO nanoparticles.

$$\text{Removal } (\%) = \frac{C_o - C_e}{C_o} \times 100 \quad (1)$$

where C_o is the initial concentration of chromium (VI) and C_e is the equilibrium concentration of chromium (VI).

3.2.1. Effect of pH

The removal of chromium (VI) was carried out in pH range 1.0–6.0 using adsorbent CdO and modified CdO nanoparticles (0.200 g/50 ml) keeping chromium (VI) concentration constant as 200 mg/l (Fig. 9(a)). The adsorption of chromium (VI) was not significant at pH values more than pH 6.0 [62]. The pH of the chromium (VI) solution was adjusted using sulfuric acid (2.0 M) and sodium hydroxide (2.0 M). The rate of removal of chromium (VI) increases with increasing pH up to 3.0 and above this it shows decrease in the rate of removal of chromium (VI). The maximum removal of chromium (VI) occurs at pH 3.0. The influence of pH of the initial solution on the chromium

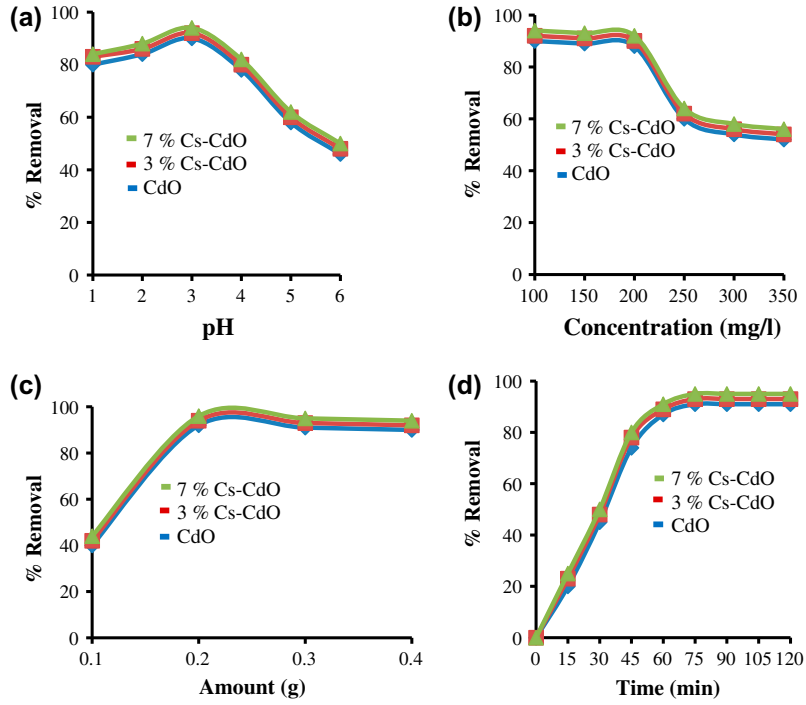

Fig. 9. Removal of chromium (a) effect of pH, (b) effect of chromium concentration, (c) effect of nature and amount of adsorbent, and (d) effect of contact time.

(VI) adsorption is explained by the ionic state of the functional groups from CdO and modified CdO nanoparticles involved in metal binding as well as by the occurrence of the hydrated cation [Cr(VI)] as a predominant ionic species [63,64]. At low pH, the competition between the H^+ ions and chromium (VI) ions for the adsorption sites of CdO and modified CdO nanoparticles causes low adsorption. By increasing initial pH, the dissociation degree of the hydroxyl groups and the negative charge density on the CdO and modified CdO nanoparticles surface are increasing resulting in a higher adsorption ratio by the electrostatic interaction with cation. After the optimum pH, the negative charge density goes on increasing due to which decrease in adsorption of chromium.

3.2.2. Effect of concentration of chromium (VI)

The removal of chromium (VI) was carried out with 100–350 mg/l initial concentration of chromium (VI) using different adsorbent such as CdO and Cs-doped CdO nanoparticles with amount of 0.200 g/50 ml and at pH 3.0 (Fig. 9(b)). The rate of removal of chromium (VI) is more up to 200 mg/l and further increase in concentration of chromium (VI) the rate of removal of chromium (VI) decreases. During the increase in initial concentration of chromium (VI), the surface area of CdO and Cs-doped CdO nanoparticles available for the adsorption is not sufficient therefore, the rate of removal of chromium decreases with increase in concentration of chromium (VI). In previous work [25,42,45] smaller amount of chromium has been removed (VI), while in present work maximum removal of chromium has been achieved with initial concentration 200 mg/l.

3.2.3. Effect of amount of CdO nanoparticles

The amount of adsorbent affects the rate of removal of chromium (VI) hence different amounts of CdO and modified CdO nanoparticles were used for the removal of chromium (VI) (Fig. 9(c)). The result shows that the rate of removal of chromium (VI) increases with increase in the amount of CdO and Cs-doped CdO nanoparticles but it remains constant after a 0.200 g/50 ml amount. This may be due to that, as the amount of CdO and modified CdO nanoparticles was increased, the exposed surface area also increases but after certain limit with the increase in CdO and modified CdO nanoparticles, there will be no increase in the exposed surface area of the adsorbent. It may be considered like a saturation point, the increase in the amount of CdO and modified CdO nanoparticles after this saturation point will only increase the thickness of the layer at the bottom of the reaction vessel. The removal efficiency is directly

related to the number of active sites available. After certain amount of adsorbent, the maximum adsorption sets hence the amount of ions bound to the adsorbent and the free ions remains constant even with further addition of the adsorbent. In earlier reported work [24,25], large amount of adsorbent has been required to remove the chromium from the solution; however in present work, 0.200 g/50 ml of adsorbent has been sufficient to remove maximum chromium (VI) from aqueous solution.

3.2.4. Effect of nature of CdO nanoparticles

Adsorption phenomenon was carried out with adsorbent such as CdO and Cs-doped CdO with chromium (VI) concentration solution 200 mg/l to study the nature of adsorbent on removal of chromium (VI). The removal of chromium (VI) was more with Cs-doped CdO nanoparticles than undoped CdO nanoparticles (Fig. 9(c)). The Cs-doped CdO nanoparticles have large surface area as compared to undoped CdO nanoparticles; therefore, Cs-doped CdO nanoparticles are more effective as compared to undoped CdO nanoparticles. In semiconductor–electrolyte interface with light energy greater than the semiconductor band gap, electron-hole pairs (e^-/h^+) are formed in the conduction and the valence band of the semiconductor, respectively [65]. These charge carriers which migrate to the semiconductor surfaces are capable of reducing or oxidizing species in solution having suitable redox potential. As compared to previous work [24], 97% of chromium has been removed from aqueous solution using CdO and modified CdO nanoparticles.

3.2.5. Effect of contact time

The effect of the contact time for the removal of chromium (VI) from the aqueous solution using CdO or modified CdO nanoparticles was analyzed under keeping the initial concentration 200 mg/l of chromium (VI), pH 3.0, and adsorbents 0.200 g/50 ml as constant. The removal of chromium was studied at different time intervals. The percent of removal increases with time and attains equilibrium at 60 min (Fig. 9(d)). However, it remains constant after an equilibrium time of 60 min, which indicates that the adsorption tends toward saturation.

3.2.6. Determination of zero point charge (ZPC)

The adsorption of chromium by CdO and modified CdO nanoparticles (0.200 g/50 ml) was carried out up to 48 h for the investigation of ZPC of CdO and modified CdO nanoparticles [66]. The values of the initial and final pH were plotted at 24 and 48 h time intervals for the CdO and modified CdO nanoparticles (Fig. 10). The point at which initial pH and final pH is equal gives ZPC for CdO and modified CdO nanoparticles (Table 1). The ZPC for CdO and modified CdO nanoparticles are 6.00.

3.2.7. Maximum removal of chromium (VI)

The adsorption characteristics of CdO and modified CdO nanoparticles have been studied with respect to pH, initial concentration of chromium (VI), amount of adsorbent, and nature of adsorbent. The maximum removal of chromium (VI) was found to be at pH 3.0. An initial concentration of chromium (VI) was also affect the removal efficiency and maximum removal

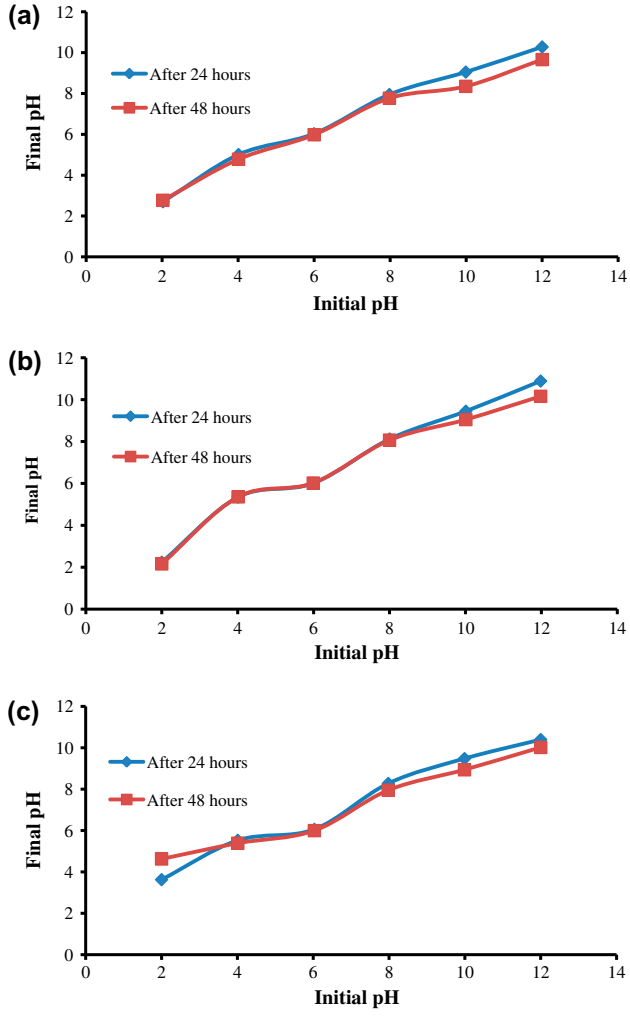

Fig. 10. Zero point charge of (a) CdO, (b) 3% Cs-doped CdO, and (c) 7% Cs doped CdO.

Table 1
Zero point charge of CdO and modified CdO nanoparticles

Adsorbent	Amount (g)	Initial pH	Final pH	
			After 24 h	After 48 h
CdO	0.200	2.02	2.70	2.77
	0.200	4.01	5.01	4.78
	0.200	6.00	6.03	5.98
	0.200	7.98	7.95	7.77
	0.200	9.99	9.05	8.35
	0.200	12.00	10.28	9.66
3% Cs–CdO	0.200	2.00	2.24	2.16
	0.200	4.01	5.35	5.36
	0.200	5.99	6.01	6.02
	0.200	8.00	8.12	8.07
	0.200	10.01	9.45	9.05
	0.200	11.98	10.89	10.16
7% Cs–CdO	0.200	2.00	3.63	4.63
	0.200	4.01	5.53	5.39
	0.200	6.03	6.06	6.00
	0.200	7.98	8.28	7.95
	0.200	9.99	9.48	8.94
	0.200	12.00	10.40	10.02

occurs at 200 mg/l concentration of chromium. The removal efficiency was related to the amount of adsorbent and 0.200 g/50 ml amount of CdO or modified CdO nanoparticles was sufficient for the maximum removal. The modified CdO nanoparticles have more removal efficiency towards chromium (VI) due to its high surface area (Table 2).

3.2.8. Removal of the chromium (VI) from wastewater

The chromium (VI) was removed from treated wastewater using CdO and modified CdO nanoparticles (0.200 g/50 ml, pH 3.0). The removal of chromium (VI) was tested by measuring absorbance of wastewater using UV–visible spectrophotometer. Concentration of chromium (VI) in the treated waste water before and after was also determined by Atomic Absorption Spectrometry (Chemito AA203) an air–acetylene burner. The result shows that 93% of chromium was removed from treated wastewater with modified CdO nanoparticles (Table 3).

3.3. Adsorption isotherm

The synthesized nanoparticles CdO and modified CdO are considered to have significant capability to adsorb heavy metals. From the study of adsorption at different condition, the Langmuir and Freundlich adsorption isotherm [67,68] parameters are to be evaluated.

3.3.1. Langmuir isotherm

The validity of Langmuir adsorption isotherm is tested by plotting $C_e/(x/m)$ against C_e. Where x = the mass of solute adsorbed, m = mass of adsorbent, x/m = the mass of solute adsorbed per unit mass of adsorbent, and C_e = the equilibrium concentration of the adsorbed substance in the solution. The characteristic of Langmuir isotherm model can be described by separation factor [64] as follows,

$$R_L = 1 / (1 + b\, C_o) \quad (2)$$

Table 2
Parameters for the maximum removal of chromium (VI)

Sr. no.	Parameters	Optimum value
1	pH	3.0
2	Initial concentration of Cr(VI)	200 mg/l
3	Amount of adsorbent	0.200 g/50 ml
4	Nature of adsorbent	7% Cs—CdO nanoparticles

Table 3
Removal of chromium from treated waste water

Sr. no.	Concentration of chromium (mg/l)	Meter reading
1	00	00
2	10	19
3	20	40
4	30	61
5	40	80
6	50	100
7	Sample 1	89
8	Sample 2	11
9	Sample 3	08
10	Sample 4	06

Notes: Sample 1: Before removal of chromium.
Sample 2: After removal of chromium with CdO nanoparticles.
Sample 3: After removal of chromium with 3% Cs–CdO nanoparticles.
Sample 4: After removal of chromium with 7% Cs–CdO nanoparticles.

where b is the Langmuir constant (Fig. 10) and C_o is the initial concentration of chromium (VI) ion. The adsorption process is thermodynamically unfavorable, if $R_L > 1$, linear if $R_L = 1$, thermodynamically favorable if $0 < R_L < 1$ and irreversible if $R_L = 0$. In these adsorption experiments, calculated R_L value is in the range 0.0204–0.0311, therefore the adsorption process is thermodynamically favorable. The adsorption capacity of 7% Cs doped CdO nanoparticles is more to that of CdO nanoparticles which is due to the surface area of 7% Cs-doped CdO nanoparticles is more than that of undoped CdO nanoparticles.

3.3.2. Freundlich isotherm

The applicability of Freundlich adsorption isotherm is tested by plotting log (x/m) against log C_e. Where x = the mass of solute adsorbed, m = mass of adsorbent, x/m = the mass of solute adsorbed per unit mass of adsorbent, and C_e = the equilibrium concentration of the adsorbed substance in the solution. The

Table 4
Langmuir and Freundlich adsorption isotherm parameters

	Langmuir parameters			Freundlich parameters		
Adsorbent	b	a	R^2	n	K_f	R^2
CdO	0.155	0.125	0.950	1.865	0.034	0.980
3% Cs—CdO	0.199	0.136	0.976	1.779	1.206	0.985
7% Cs—CdO	0.239	0.164	0.991	1.748	1.237	0.992

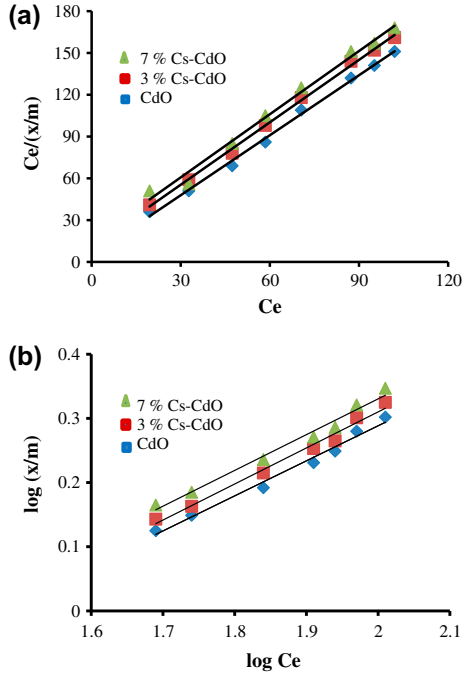

Fig. 11. (a) Langmuir adsorption isotherm and (b) Freundlich adsorption isotherm.

Freundlich isotherm constants (K_f and n) calculated from Fig. 11 and given in Table 4. The R^2 value for the adsorption of chromium (VI) is obtained from Fig. 11, fits for Freundlich isotherm very well. The "n" value for adsorption of the chromium (VI) is greater than 1, revealing that adsorption was a favorable process.

4. Conclusions

The present work reports the removal of chromium (VI) using CdO and modified CdO nanoparticles. The result indicates that, modified CdO nanoparticles were more efficient than CdO nanoparticles as adsorbent for removal of chromium (VI). The maximum removal of chromium (VI) is 0.200 g/50 ml amount of adsorbents in 60 min at pH 3.0. It was found that Freundlich isotherm model was more obeyed. The method was successfully applicable for removal of chromium (VI) from wastewater samples.

Acknowledgments

We are thankful to CSIR, New Delhi (01/2745/13/EMR-II) and BCUD, Savitribai Phule Pune University for financial assistance. The authors are thankful to Principal, HPT Arts and RYK Science College, Nasik for providing necessary laboratory facilities.

We would also acknowledge department of Physics, Savitribai Phule Pune University for providing characterization facilities. Authors are thankful to Prof. D.G. Thorat and Dr. Anil G. Gadhave for his helpful suggestions.

List of abbreviations

UV–DRS	—	ultra violet–visible reflectance spectroscopy
FT-IR	—	Fourier Transform-Infra red spectroscopy
XRD	—	X-ray diffraction analysis
SEM	—	scanning electron microscopy
EDAX	—	energy dispersive X-ray spectroscopy
TEM	—	transmission electron microscopy
SAED	—	selected area electron diffraction spectroscopy
TGA	—	thermogravimetric analysis
PL	—	photoluminescence analysis
BET	—	Brunauer–Emmett–Teller surface area analysis
BJH	—	Barrett–Joyner–Halenda Analysis
ppm	—	part per million
M	—	molar
N	—	normal
mol	—	mole
mmol	—	millimole
mg/l	—	milligrams per liter
g	—	gram
ZPC	—	zero point charge
S_{BET}	—	specific surface area
V_p	—	pore volume (m^2/g)
m^2/g	—	meter square per gram
d_p	—	pore diameter (cc/g)
cc/g	—	cubic centimeter per gram
E	—	band gap energy (eV)
C_o	—	initial concentration of chromium (mg/l)
C_e	—	equilibrium concentration of chromium (mg/l)
K_f	—	Freundlich constant (mg/g)
n	—	Freundlich constants (mg/g)
b	—	Langmuir constant (mg/g)
a	—	Langmuir constant (mg/g)
R^2	—	correlation coefficient
x	—	mass of solute
x/m	—	mass of solute adsorbed per unit mass of adsorbent
R_L	—	separation factor

References

[1] A. Gulino, G. Compagnini, A.A. Scalisi, Large third-order nonlinear optical properties of cadmium oxide thin films, Chem. Mater. 15 (2003) 3332–3336.
[2] D.R. Lide, Chemical Rubber Company Handbook of Chemistry and Physics, seventyseventh ed, CRC Press, Boca Raton, FL, USA, 1996.
[3] J.H. Bang, K.S. Suslick, Sonochemical synthesis of nanosized hollow hematite, J. Am. Chem. Soc. 129 (2007) 2242–2243.
[4] P.K. Ghosh, S. Das, S. Kundoo, K.K. Chattopadhyay, Effect of fluorine doping on semiconductor to metal-like transition and optical properties of cadmium oxide thin films deposited by sol–gel process, J. Sol-Gel Sci. Technol. 34 (2005) 173–179.
[5] D.S. Dhawale, A.M. More, S.S. Latthe, K.Y. Rajpure, C.D. Lokhande, Room temperature synthesis and characterization of CdO nanowires by chemical bath deposition (CBD) method, Appl. Surf. Sci. 254 (2008) 3269–3273.
[6] M. Zaien, N.M. Ahmed, Z. Hassan, Growth of cadmium oxide nano rods by vapor transport, Chalcogenide Lett. 9 (2012) 115–119.
[7] M. Zaien, K. Omar, Z. Hassan, Growth of nanostructured CdO by solid–vapor deposition, Int. J. Phys. Sci. 6 (2011) 4176–4180.
[8] A.S. Lanje, R.S. Ningthoujam, S.J. Sharma, R.B. Pode, Luminescence and electrical resistivity properties of cadmium oxide nanoparticles, Indian J. Pure Appl. Phys. 49 (2011) 234–238.
[9] J.K. Andeani, S. Mohsenzadeh, Photosynthesis of cadmium oxide nanoparticles from *Achillea wilhelmsii* flowers, J. Chem. (2013), doi: 10.1155/2013/147613 (Article ID 147613).
[10] M. Ghosh, C.N.R. Rao, Solvothermal synthesis of CdO and CuO nanocrystals, Chem. Phys. Lett. 393 (2004) 493–497.
[11] A. Tadjarodi, M. Imani, Synthesis and characterization of CdO nanocrystalline structure by mechanochemical method, Mater. Lett. 65 (2011) 1025–1027.
[12] P.A. Radi, A.G. Brito-Madurro, J.M. Madurro, N.O. Dantas, Characterization and properties of CdO nanocrystals incorporated in polyacrylamide, Braz. J. Phys. 36 (2006) 412–414.
[13] K. Byrappa, T. Adschiri, Hydrothermal technology for nanotechnology, Prog. Cryst. Growth Charact. Mater. 53 (2007) 117–166.
[14] A.A. Dakhel, F.Z. Henari, Optical characterization of thermally evaporated thin CdO films, Cryst. Res. Technol. 38 (2003) 979–985.
[15] W. Dong, C. Zhu, Optical properties of surface-modified CdO nanoparticles, Opt. Mater. 22 (2003) 227–233.
[16] K.M. Abd El-Salaam, E.A. Hassan, Active surface centres in a heterogeneous CdO catalyst for ethanol decomposition, Surf. Technol. 16 (1982) 121–128.
[17] S. Reddy, B.E.K. Swamy, U. Chandra, B.S. Sherigara, H. Jayadevappa, Synthesis of CdO nanoparticles and their modified carbon paste electrode for determination of dopamine and ascorbic acid by using cyclic voltammetry technique, Int. J. Electrochem. Sci. 5 (2010) 10–17.
[18] M. Shukla, S. Kumari, S. Shukla, R.K. Shukla, Potent antibacterial activity of nano CdO synthesized via microemulsion scheme, J. Mater. Environ. Sci. 3(4) (2012) 678–685.
[19] R.H. Wang, J.H. Xin, X.M. Tao, W.A. Daoud, ZnO Nanorods grown on cotton fabrics at low temperature, Chem. Phys. Lett. 398 (2004) 250–255.
[20] M. Mazaheritehrani, J. Asghari, R.L. Orimi, S. Pahlavan, Microwave-assisted synthesis of nanosized cadmium oxide as anew and highly efficient catalyst for solvent

free acylation of amines and alcohols, Asian J. Chem. 22 (2010) 2554–2564.
[21] W. Weilong, F. Xiaobo, Efficient removal of chromium (VI) with Fe/Mn mixed metal oxide nanocomposites synthesized by a grinding method, J. Nanomater. (2013), doi: 10.1155/2013/514917 (Article ID 514917).
[22] S. Singh, K.C. Barick, D. Bahadur, Fe_3O_4 embedded ZnO nanocomposites for the removal of toxic metal ions, organic dyes and bacterial pathogens, J. Mater. Chem. A 1 (2013) 3325–3333.
[23] X.S. Wang, Z.Z. Li, S.R. Tao, Removal of chromium (VI) from aqueous solution using walnut hull, J. Environ. Manage. 90 (2009) 721–729.
[24] E. Pehlivan, T. Altun, Biosorption of chromium (VI) ion from aqueous solutions using walnut, hazelnut and almond shell, J. Hazard. Mater. 155 (2008) 378–384.
[25] N. Ertugay, Y.K. Bayhan, Biosorption of Cr (VI) from aqueous solutions by biomass of Agaricus bisporus, J. Hazard. Mater. 154 (2008) 432–439.
[26] F.B. Liang, Y.L. Song, C.P.H. Huang, J. Zhang, Adsorption of hexavalent chromium on a lignin-based resin: Equilibrium, thermodynamics and kinetics, J. Envrion. Chem. Eng. 1 (2013) 1301–1308.
[27] N.V. Nguyen, J.C. Lee, J. Jeong, B.D. Pandey, Enhancing the adsorption of chromium (VI) from the acidic chloride media using solvent impregnated resin (SIR), Chem. Eng. J. 219 (2013) 174–182.
[28] A.B. Albadarin, C. Mangwandi, A.H. Al-Muhtaseb, G.M. Walker, S.J. Allen, M.N.M. Ahmad, Kinetic and thermodynamics of chromium ions adsorption onto low-cost dolomite adsorbent, Chem. Eng. J. 179 (2012) 193–202.
[29] A.V. Bankar, A.R. Kumar, S.S. Zinjarde, Removal of chromium (VI) ions from aqueous solution by adsorption onto two marine isolates of Yarrowia lipolytica, J. Hazard. Mater. 170 (2009) 487–494.
[30] V. Marjanović, S. Lazarević, I. Janković-Častvan, B. Jokić, D. Janaćković, R. Petrović, Adsorption of chromium(VI) from aqueous solutions onto amine-functionalized natural and acid-activated sepiolites, Appl. Clay Sci. 80-81 (2013) 202–210.
[31] C. Jung, J. Heo, J. Han, N. Her, S.J. Lee, J. Oh, J. Ryu, Y. Yoon, Hexavalent chromium removal by various adsorbents: Powdered activated carbon, chitosan and single/multi-walled carbon nanotubes, Sep. Purif. Technol. 106 (2013) 63–71.
[32] J. Wang, K. Pan, Q. He, B. Cao, Polyacrylonitrile/polypyrrole core/shell nanofiber mat for the removal of hexavalent chromium from aqueous solution, J. Hazard. Mater. 244-245 (2013) 121–129.
[33] H. Deveci, Y. Kar, Adsorption of hexavalent chromium from aqueous solutions by bio-chars obtained during biomass pyrolysis, J. Ind. Eng. Chem. 19 (2013) 190–196.
[34] D. Chauhan, M. Jaiswal, N. Sankararamakrishnan, Removal of cadmium and hexavalent chromium from electroplating waste water using thiocarbamoyl chitosan, Carbohydr. Polym. 88 (2012) 670–675.
[35] D.D. Maksin, A.B. Nastasović, A.D. Milutinović-Nikolić, L.T. Suručić, Z.P. Sandić, R.V. Hercigonja, A.E. Onjia, Equilibrium and kinetics study on hexavalent chromium adsorption onto diethylene triamine grafted glycidyl methacrylate based copolymers, J. Hazard. Mater. 209–210 (2012) 99–110.
[36] M. Hua, S. Zhang, B. Pan, W. Zhang, L. Lv, Q. Zhang, Heavy metal removal from water/wastewater by nanosized metal oxides: A review, J. Hazard. Mater. 211–212 (2012) 317–331.
[37] X. Xu, B.Y. Gao, X. Tan, Q.Y. Yue, Q.Q. Zhong, Q. Li, Characteristics of amine-crosslinked wheat straw and its adsorption mechanisms for phosphate and chromium (VI) removal from aqueous solution, Carbohydr. Polym. 84 (2011) 1054–1060.
[38] V.K. Gupta, A. Rastogi, A. Nayak, Adsorption studies on the removal of hexavalent chromium from aqueous solution using a low cost fertilizer industry waste material, J. Colloid Interface Sci. 342 (2010) 135–141.
[39] O.S. Amuda, F.E. Adelowo, M.O. Ologunde, Kinetics and equilibrium studies of adsorption of chromium (VI) ion from industrial wastewater using Chrysophyllum albidum (Sapotaceae) seed shells, Colloids Surf. B 68 (2009) 184–192.
[40] M. Barkat, D. Nibou, S. Chegrouche, A. Mellah, Kinetics and thermodynamics studies of chromium (VI) ions adsorption onto activated carbon from aqueous solutions, Chem. Eng. Process. Process Intensif. 48 (2009) 38–47.
[41] M.S. Gasser, G.A. Morad, H.F. Aly, Batch kinetics and thermodynamics of chromium ions removal from waste solutions using synthetic adsorbents, J. Hazard. Mater. 142 (2007) 118–129.
[42] F. Gode, E. Pehlivan, Removal of Cr(VI) from aqueous solution by two Lewatit-anion exchange resins, J. Hazard. Mater. 119 (2005) 175–182.
[43] S. Rengaraj, K.H. Yeon, S.H. Moon, Removal of chromium from water and wastewater by ion exchange resins, J. Hazard. Mater. 87 (2001) 273–287.
[44] B. Singha, T.K. Naiya, A.K. Bhattacharya, S.K. Das, Cr(VI) ions removal from aqueous solutions using natural adsorbents—FTIR studies, J. Environ. Prot. 02 (2011) 729–735.
[45] N. Li, J. Ren, L. Zhao, Z.L. Wang, Removal of Cr(VI) ions from wastewater using nanosized ferric oxyhydroxide loaded anion exchanger on a fixedbed column, Desalin. Water Treat. 52(19–21) (2014) 3572–3578.
[46] S. Kumar, B.C. Meikap, Removal of Chromium(VI) from waste water by using adsorbent prepared from green coconut shell, Desalin. Water Treat. 52(16–18) (2014) 3122–3132.
[47] Z. Zhu, Y. Zhu, F. Yang, X. Zhang, H. Qin, Y. Liang, J. Liu, Sorption-reduction removal of Cr(VI) from aqueous solution by the porous biomorph-genetic composite of α-Fe_2O_3/Fe_3O_4/C with eucalyptus wood hierarchical microstructure, Desalin. Water Treat. 52 (16–18) (2014) 3133–3146.
[48] A. Olad, F.F. Farshi Azhar, A study on the adsorption of chromium (VI) from aqueous solutions on the alginate-montmorillonite/polyaniline nanocomposite, Desalin. Water Treat. 52(13–15) (2014) 2548–2559.
[49] H. Li, Z. Chi, J. Li, Covalent bonding synthesis of magnetic graphene oxide nanocomposites for Cr(III) removal, Desalin. Water Treat. 52(10–12) (2014) 1937–1946.
[50] S. Ghrab, N. Boujelbene, M. Medhioub, F. Jamoussi, Chromium and nickel removal from industrial wastewater using Tunisian clay, Desalin. Water Treat. 52(10–12) (2014) 2253–2260.

[51] U. S. Environmental Protection Agency (USEPA), Code of Federal Regulations, 40, CFR 141.32, 1999.
[52] Agency for Toxic Substances and Disease Registry (ATSDR), Toxicological Profile for Chromium, U. S. Department of Health and Human Services, Public Health Service, Atlanta, GA, 2000.
[53] V.K. Gupta, A. Rastogi, Sorption and desorption studies of chromium(VI) from nonviable cyanobacterium Nostoc muscorum biomass, J. Hazard. Mater. 154(1–3) (2008) 347–354.
[54] F.N. Acar, E. Malkoc, The removal of chromium(VI) from aqueous solutions by Fagus orientalis L, Bioresour. Technol. 94 (2004) 13–15.
[55] A.V. Borhade, B.K. Uphade, A.G. Gadhave, Efficient, solvent free synthesis of acridinediones catalyzed by CdO nanoparticles, Res. Chem. Intermed. 41(3) (2015) 1447–1458.
[56] A.I. Trokhimets, Frequency limits of valence vibrations of free -OH groups for several oxygen compounds, J. Appl. Spectrosc. 44 (1986) 88–91.
[57] J. Liu, C. Zhao, Z. Li, L. Yu, Y. Li, S. Gu, A. Cao, W. Jiang, J. Liu, C. Yang, Solid-state synthesis and optical properties-controlling studies of CdO nanoparticles, Adv. Mater. Res. 228-229 (2011) 580–585.
[58] N. Faleni, M.J. Moloto, Effect of glucose as stabilizer of ZnO and CdO nanoparticles on the morphology and optical properties, Int. J. Res. Rev. Appl. Sci. 14 (2013) 127–135.
[59] N.S. Gajbhiye, R.S. Ningthoujam, A. Ahmed, S.S. Umre, S.J. Sharma, D.K. Panda, Re-dispersible Li^{+} and Eu^{3+} Co-doped CdO nanowires: Luminescence studies: 9th Asian Symposium on Information Display (ASID 2006), New Delhi, October, 8–12, 2006.
[60] P.K. Dash, Y. Balto, Generation of nano-copper particles through wire explosion method and its characterization, Res. J. Nanosci. Nanatechnol. 1 (2011) 25–33.
[61] M.C.M. Alvim Ferraz, S. Möser, M. Tonhäeuser, Control of atmospheric emissions of volatile organic compounds using impregnated active carbons, Fuel. 78 (1999) 1567–1573.
[62] S. Mallick, S.S. Dash, K.M. Parida, Adsorption of hexavalent chromium on manganese nodule leached residue obtained from NH_3–SO_2 leaching, J. Colloid Interface Sci. 297 (2006) 419–425.
[63] A. Sen, M.A. Olivella, N. Fiol, I. Miranda, I. Villaescusa, H. Pereira, Removal of chromium (VI) in aqueous environments using cork and heat treated cork samples from Quercus cerris and Quercus suber, Bioresources. 7 (4) (2012) 4843–4857.
[64] A. Kannan, S. Thambidurai, Removal of hexavalent chromium from aqueous solution using activated carbon derived from Palmyra palm fruit seed, Bull. Chem. Soc. Ethiop. 22(2) (2008) 183–196.
[65] J.M. Herrmann, Heterogeneous photocatalysis fundamentals and applications to the removal of various types of aqueous pollutants, Catal. Today 53 (1999) 115–129.
[66] G. Mustafa, H. Tahir, M. Sultan, N. Akhtar, Synthesis and characterization of cupric oxide (CuO) nanoparticles and their application for the removal of dyes, Afr. J. Biotechnol. 12 (2013) 6650–6660.
[67] I. Langmuir, The constitution and fundamental properties of solids and liquids. Part I. Solids, J. Am. Chem. Soc. 38 (1916) 2221–2295.
[68] H.M.F. Freundlich, Uber die adsorption in losungen (adsorption in solution), Z. Phys. Chem. 57 (1906) 385–470.